Chinese Chemical Letters 37 (2026) 111134

Contents lists available at ScienceDirect

Chinese Chemical Letters

journal homepage: www.elsevier.com/locate/cclet

Facile and scale-up synthesis of cyano-functionalized covalent organic frameworks for selective gold recovery

Bo Li[a,b], Yuanzhe Cheng[a], Xuyang Ma[a], Dongxu Zhao[a], Yang Zhang[a], Yongxing Sun[b], Jia Chen[b,*], Li Wu[a], Liang Zhao[b], Hongdeng Qiu[b,*], Yujian He[a,*]

[a] School of Chemical Sciences, University of Chinese Academy of Sciences, Beijing 100049, China
[b] CAS Key Laboratory of Chemistry of Northwestern Plant Resources and Key Laboratory for Natural Medicine of Gansu Province, Lanzhou Institute of Chemical Physics, Chinese Academy of Sciences, Lanzhou 730000, China

ARTICLE INFO

Article history:
Received 9 January 2025
Revised 11 March 2025
Accepted 20 March 2025
Available online 20 March 2025

Keywords:
Cyano functionalization
Gold recovery
Covalent organic frameworks
Waste electronic and electric equipment
Selectivity

ABSTRACT

The recovery of gold from waste electronic and electric equipment (WEEE) has gained great attention with the increased number of WEEE, because it can largely alleviate the pressure on the environment and resources. Covalent organic frameworks (COFs) are ideal adsorbents for gold recovery owing to their large surface area, good stability, easily functionalized ability, periodic structures, and definitive nanopores. Herein, a cyano-functionalized COF (COF-CN) with high crystallinity was large-scale prepared under mild conditions for the recovery of gold. The introduction of cyano groups enable COF-CN to exhibit excellent gold recovery performance, which possesses fast adsorption kinetics, high cycling stability, and adsorption capacity up to 663.67 mg/g. Excitingly, COF-CN showed extremely high selectivity for gold ions, even in the presence of various competing cations and anions. The COF-CN maintained excellent selectivity and removal efficiency in gold recovery experiments from WEEE. The facile synthesis of COF-CN and its outstanding selectivity in actual samples make it an attractive opportunity for practical gold recovery.

© 2025 Published by Elsevier B.V. on behalf of Chinese Chemical Society and Institute of Materia Medica, Chinese Academy of Medical Sciences.

Gold, one of the rarest and most precious metals, is essential for modern technology but faces severe resource scarcity due to the ever-growing demand and finite natural reserves [1]. Traditional primary gold mining is cumbersome, environmentally damaging, and inefficient, while the gold content in waste electrical and electronic equipment (WEEE) is 80 times greater than that found in primary gold mining worldwide [2,3]. On the other hand, the generation of WEEE has emerged as one of the fastest-growing wastes, causing serious environmental and economic problems [4,5]. Importantly, traditional methods of collecting and disposing e-waste significantly increase harmful substances [6,7]. Thus, designing effective methods to recover gold from WEEE will solve the resource scarcity dilemma and alleviate environmental problems.

Among gold recovery methods, adsorption is viewed as the most promising method for gold recovery owing to its high efficiency, simplicity, reusability and low cost [8]. Many adsorbents have been reported, such as biomass materials [9], silica-based materials [10], carbon materials [11], and metal organic frameworks (MOFs) [12]. However, these adsorbents involve several disadvantages, such as the lack of sufficient functional groups, poor selectivity, long adsorption time, and weak reusability. Therefore, designing prominent adsorbents with excellent adsorption performance is essential for selectively recovering gold from WEEE.

Covalent organic frameworks (COFs) represent a class category of crystalline porous materials linked by the covalent bonding of organic monomers [13]. The high porosity, large surface area, long-range ordered structure have positioned COFs at the forefront of materials science research, leading to their extensive application in various fields [14–16]. Moreover, various functionalized units can be introduced into highly ordered periodic arrays, allowing for precise assembly based on the principles of reticulate chemistry [17]. Up to now, multi-adsorption sites are introduced into COFs as functional groups such as thiol [18], amide [19], hydroxyl [8,20], and these functionalized COFs [21,22] have shown good performance in gold recovery.

However, the preparation of these COFs is often complex, necessitating toxic organic solvents or high-pressure/high-temperature conditions, and typically yielding less than 100 mg in single-batch reactions. Additionally, some COFs require intricate pre- or post-treatments [23]. It is very significant to find a mild method to prepare functionalized COF on a large scale for practical gold recovery.

* Corresponding authors.
E-mail addresses: jiachen@licp.cas.cn (J. Chen), hdqiu@licp.cas.cn (H. Qiu), heyujian@ucas.ac.cn (Y. He).

https://doi.org/10.1016/j.cclet.2025.111134
1001-8417/© 2025 Published by Elsevier B.V. on behalf of Chinese Chemical Society and Institute of Materia Medica, Chinese Academy of Medical Sciences.

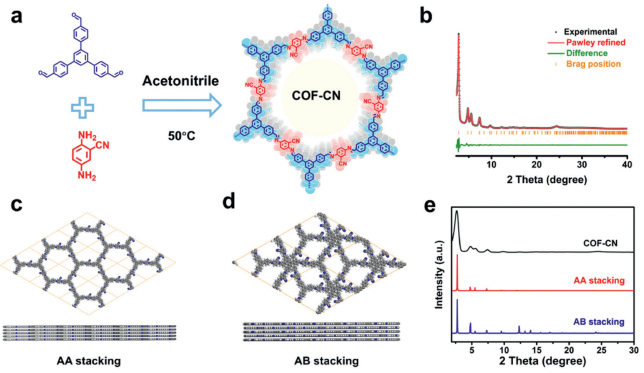


Fig. 1. (a) The schematic route of synthesis COF-CN. (b) PXRD profiles of COF-CN. (c, d) Top view and side view of AA and AB stacked models and (e) the corresponding PXRD patterns.

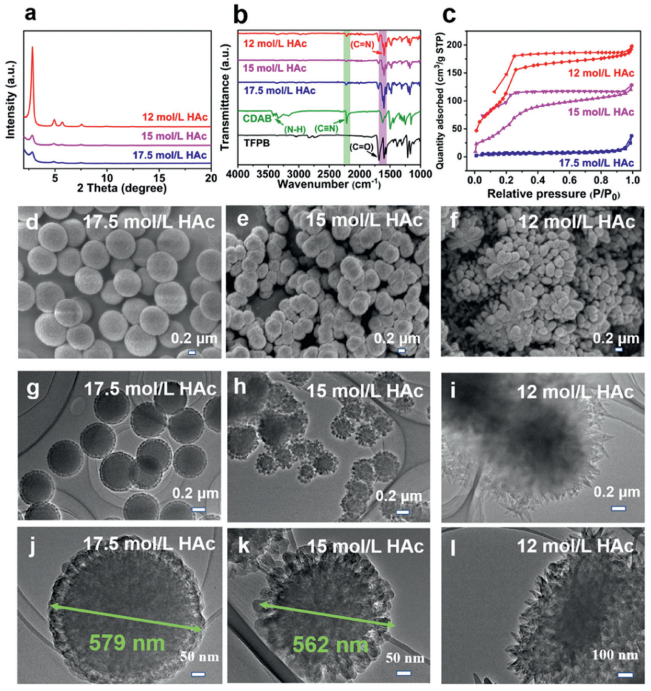


Fig. 2. (a) The PXRD patterns of COF-CN prepared at different concentrations of HAc. (b) FT-IR spectra of COF-CN prepared at different concentrations of HAc, and the building block of TFPB and CDAB. (c) N_2 absorption/desorption experiments results. SEM and TEM images of COF-CN prepared at different concentrations of HAc. (d, g, j) 17.5 mol/L HAc, (e, h, k) 15 mol/L HAc, and (f, i, l) 12 mol/L HAc.

In this work, the new cyano-functionalized COFs (COF-CN) were successfully designed and synthesized. Due to the introduction of cyano functional groups, the COFs with this structure can be successfully prepared under mild conditions and can reach a preparation scale of gram level. The prepared COF-CN exhibits a regular morphology, high crystallinity, good stability, and a large specific surface area. COF-CN can possess a good gold adsorption capacity of 663.67 mg/g. Excitingly, COF-CN showed extremely high selectivity for gold ions, even in the presence of various competing cations and anions. More importantly, COF-CN maintained its excellent selectivity and removal efficiency toward the central processing unit (CPU) leaching solution in gold recovery experiments.

The synthesis of COF-CN is described in Fig. 1a using the building blocks of 1,3,5-tris(*p*-formylphenyl)benzene (TFPB) and 2-cyano-1,4-diaminobenzene (CDAB). In brief, TFPB and CDAB were dissolved with acetonitrile (ACN), followed by addition of 12 mol/L HAc as the catalyst for Schiff base condensation. After reacting at 50 °C for 72 h, yellow residues were obtained by centrifugation. Powder X-ray diffraction (PXRD) analysis was carried out to assess the crystallinity of COF-CN. The results revealed a prominent diffraction peak at 2.74°, indicating strong crystallographic order within the framework materials (Fig. 1b). And several peaks are observed at 4.83°, 5.59°, 7.42°, 9.74°, which correspond to the (100), (110), (200), (120), and (220) crystal planes, respectively. In addition, a weaker peak at 25.78° has been noted, which comes from the (001) side of the $\pi-\pi$ stacking accumulation. The Pawley refined profile fit well, with an R_{wp} 4.08 % and R_p only 3.06 %. To further understand the potential structure of the prepared COFs, two 2D structural models were constructed (Figs. 1c and d). As shown in Fig. 1e, the simulated XRD of the AA stacking model aligns more closely with the experimental result. Detailed cell parameters are provided in Table S1 (Supporting information). These results indicate the successful synthesis and the high crystallinity of COF-CN.

Interestingly, we observed that the concentration of the regulator HAc had significantly influences of prepared COF-CN. As shown in Fig. 2a, different crystallinity products could be obtained at HAc concentrations of 17.5, 15 and 12 mol/L, respectively. And the best crystallinity of COF was obtained at 12 mol/L. When the HAc concentration drops from 12 mol/L to 6 mol/L, no product is obtained in the reaction solution. The infrared spectra of COF-CN were compared with those of its precursors, TFPB and CDAB. As exhibited in Fig. 2b, the absorption peaks of COF-CN at 3417 cm^{-1} (–N–H) as well as 1680 cm^{-1} (–C=O) were significantly reduced compared to CDAB and TFPB. And a new characteristic peak appeared at 1600 cm^{-1}, attributed to the stretching vibration of –C=N–. This indicates that the Schiff base reaction was successfully and that the imine bond was formed. Notably, the characteristic C≡N stretching vibration occurred at 2213 cm^{-1}, suggesting the cyano groups have been introduced into synthesized COF-CN. Further validation of the functional groups was achieved using ^{13}C solid-state NMR spectroscopy, which revealed chemical shifts of 159.96 ppm for the carbon of the imine bond and 118.75 ppm for the carbon in the cyano group (Fig. S1 in Supporting information).

The surface area and porous structure of synthesized COF-CN were assessed by measuring N_2 sorption isotherms. The results revealed that with the decrease of acetic acid concentration, the surface area, pore volume and pore size structure gradually increased (Fig. 2c and Fig. S2 in Supporting information). The calculated BET surface area values were 17, 297, and 441 m^2/g, respectively, and the corresponding pore volumes were 0.052, 0.121, and 0.383 cm^3/g. It can be found that the main pore size of COF-CN is 3.1 nm at the concentration of 12 mol/L HAc, which is consistent with the theoretical value measured by Materials studio (Fig. S2). These results indicated that the concentration of HAc has a significant influence on the porosity of COF-CN.

Moreover, the concentration of the HAc also has an important effect on the morphology of COF-CN. The spherical COF-CN was obtained at 17.5 mol/L HAc concentration. It can be observed by scanning electron microscopy (SEM) (Fig. 2d) and transmission electron microscopy (TEM) (Figs. 2g and j), that the spherical COF-CN has good dispersion and homogeneity with a particle size is about 600 nm. As the concentration of HAc decreased continuously, the dispersion and uniformity of COF-CN became worse gradually (Figs. 2e, h, and k). When the concentration of HAc was 12 mol/L, the COF-CN morphology transitioned from spherical to flower-shaped, and most began to agglomerate (Figs. 2f, i, and l). Furthermore, the effect of reaction time and HAc content was also conducted (Figs. S3 and S4 in Supporting information). Through the above research, COF-CN shows high crystallinity, high specific surface area, and regular pores when the reaction condition is

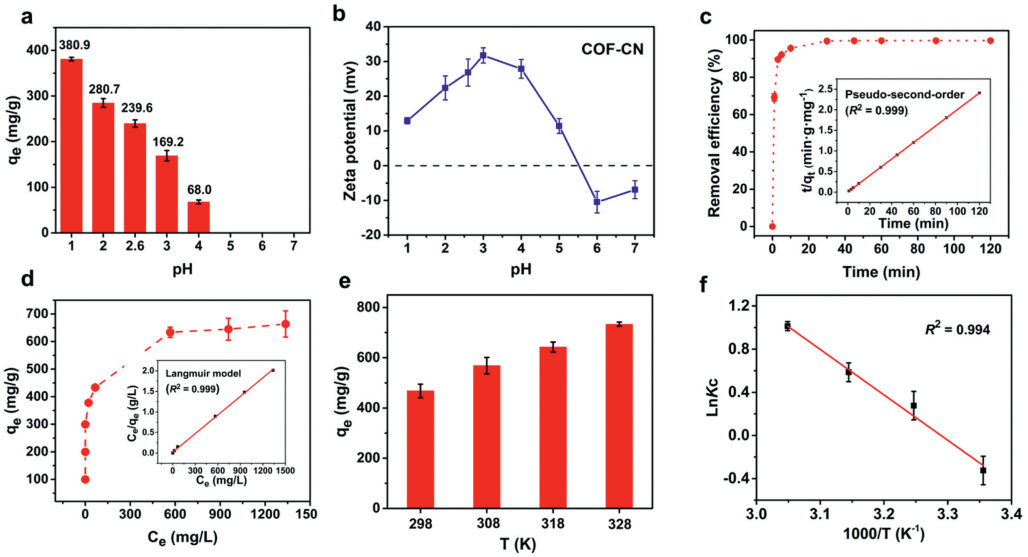


Fig. 3. (a) Adsorption capacity of COF-CN for Au(III) under different pH conditions. (b) Zeta potentials of COF-CN at different pH. (c) Adsorption kinetics of Au(III) on COF-CN. Inset: The *pseudo*-second-order model. (d) Adsorption isotherm of Au(III) on COF-CN. Inset: the Langmuir model. (e) Effect of temperature on Au(III) adsorption by COF-CN. (f) Van der Hoff plots for Au(III) adsorption of COF-CN.

12 mol/L HAc (7.2 mL) for 72 h, which are the critical factors for effective ion adsorption [17,22].

Stability is generally regarded as an important factor for the adsorbent. Thus, the chemical and thermal stability of COF-CN were further investigated. PXRD and FT-IR spectroscopic characterization revealed no significant changes in COF-CN after treatment with various concentrations of aqueous HCl solutions (Fig. S5 in Supporting information). In contrast to most imine COFs, the introduction of cyano groups improves stability in acidic environments [24]. Thermogravimetric analysis (TGA) analysis demonstrates that COF-CN exhibits excellent thermal stability up to 400 °C. These findings highlight the significant potential of COF-CN for enhancing gold recovery.

The difficulty of preparing COFs in large quantities is a key factor that restricts the practical application of COFs. The obtained products are generally at the milligram level, and when the scale of preparation is increased, the crystallinity of the prepared COFs usually decreases significantly. By scaling up the reaction by 5-fold, a single-batch synthesis produced 0.9235 g of COF-CN, approaching gram-scale production. Meanwhile, at this scale, COF-CN exhibited excellent crystallinity and a large specific surface area (Fig. S6 in Supporting information).

It is well established that the pH of the solution plays a critical role in the practical applications of gold recovery. We examined the adsorption properties and zeta potential values of COF-CN across a pH range of 1.0–7.0. Fig. 3a illustrates a steady decrease in adsorption capacity as pH increases. This phenomenon can be attributed to the hydrolysis of $AuCl_4^-$ to $Au(OH)_3$ when pH exceeds 5.0, leading to a significant increase in OH^- concentration and thereby altering the chemical composition of gold chloride complexes [21]. Meanwhile, it can also be seen that increasing Cl^- concentration does not reduce adsorption at low pH values, demonstrating that there is almost no ion exchange. Furthermore, the protonating process is more readily accessible as pH decreases, which is the key to Au(III) capture [25]. The isoelectric point of COF-CN ranges from pH 5.0 to 6.0, indicating the presence of electrostatic interactions between the COF-CN adsorbent and Au(III) ions (Fig. 3b). However, the adsorption capacity shows no significant change with zeta potential, suggesting the existence of other interactions for gold capture. Based on the previous works, we carried out adsorption experiments at pH to inhibit the reoxidation of Au(0) and the precipitation of other metal ions [26,27].

Furthermore, the adsorption kinetic of COF-CN was studied at different adsorption times. As illustrated in Fig. 3c, the adsorption performance of COF-CN shows a rapid increase at the beginning and reaches above 90 % within only 5 min. The adsorption process reached equilibrium after 30 min of adsorption time. To clarify the kinetic behaviors and adsorption mechanism of COF-CN, the results were examined using four kinetic models [28,29]. The correlation coefficients (R^2) of the four models show the following trend: *pseudo*-second-order kinetic model > intra-particle diffusion model > Elovich model > *pseudo*-first-order kinetic model. The fitting parameters of the *pseudo*-second-order kinetic model (0.999) are much larger than those of the *pseudo*-first-order kinetic model (0.439), which proves that the main adsorption behavior is mainly chemical adsorption [30]. For the intra-particle diffusion model, the R^2 values of the first and second reaction stages are 0.999 and 0.995, respectively (Fig. S7 and Table S2 in Supporting information). This indicates that the process is a rate-limiting process of external surface adsorption and intraparticle diffusion. These results show that the adsorption process in the experiment is under the control of different factors at different stages.

The adsorption isotherm of COF-CN was examined in the initial gold concentration range of 0–2000 ppm and at pH 2.0. The results were displayed in Fig. 3d and the experiment data were further fitted with Langmuir and Freundlich models. The results showed better consistency ($R^2 = 0.999$) with a theoretical maximum adsorption capacity (662.25 mg/g) predicted by the Langmuir model, closely aligning with the experiment value of 663.67 mg/g. Thus, the adsorption process is more suitable for monolayer adsorption. The fundamental parameters were computed and are detailed in Table S3 (Supporting information). This model demonstrated that the adsorption process of COF-CN for Au(III) followed the monomolecular layer adsorption behavior. Furthermore, COF-CN exhibits a superior gold adsorption capacity compared to many previously reported adsorbents (Table S4 in Supporting information), attributed to the introduction of cyano functional groups and its large specific surface area [31].

Adsorption thermodynamic experiments were performed on COF-CN to investigate the adsorption behavior (Fig. 3e). Clearly, the Au(III) adsorption capacities increased with rising temperature,

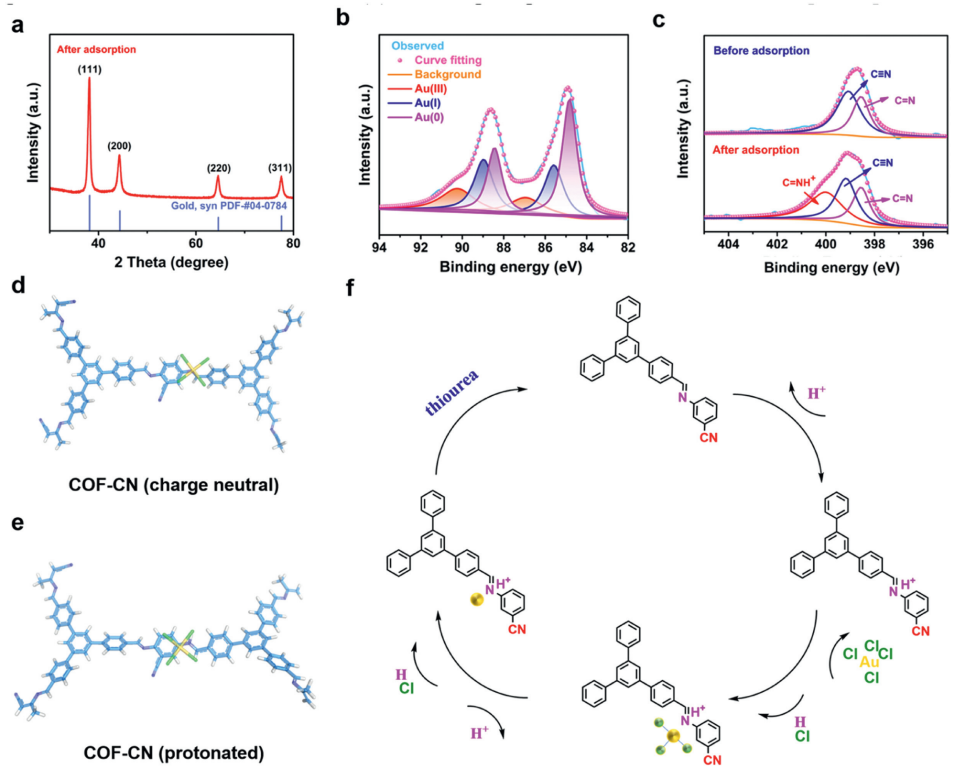


Fig. 4. (a) PXRD patterns of COF-CN after Au(III) adsorption. (b) The XPS spectra of COF-CN before and after Au(III) capture, (c) Au 4f after Au(III) adsorption and N 1s before and after the adsorption with Au(III). (d) The optimized structures for the adsorption of $AuCl_4^-$ on COF-CN and (e) protonated COF-CN. (f) The mechanism diagram of gold recovery for using COF-CN.

reaching 733.52 mg/g at 328 K. Furthermore, the thermodynamic parameters were determined using the fitting data (Fig. 3f) and the van der Hoff equations [21]. These parameters were used to assess the characteristics of the COF-CN adsorption processes. From Table S5 (Supporting information), the positive ΔS and ΔH indicated the random and endothermic characteristics of Au(III) adsorption on COF-CN. Meanwhile, the ΔG values decreased along with rising temperature, indicating that higher temperatures enhance the adsorption reaction.

To elucidate the adsorption mechanism, PXRD analysis was firstly conducted on the COF-CN after adsorption. Fig. 4a reveals the emergence of new peaks at 38.4°, 44.4°, 64.7°, and 77.6°, corresponding to the standard peaks of Au(0). The TEM image reveals that the skeleton of COF-CN is maintained well after adsorption (Fig. S8a in Supporting information). In addition, new lattice fringes were observed in the high-resolution TEM (HRTEM) image. The lattice spacings of the regularly arranged lattice stripes are 0.21 nm and 0.23 nm, corresponding to the (111) and (200) crystal facets of the Au nanoparticles, proving the formation of Au(0), which is consistent with the XRD result (Fig. S8b in Supporting information). The EDS mapping images of COF-CN after Au(III) capture show gold particles well dispersed in the skeleton (Fig. S8c in Supporting information). These results demonstrated the spontaneous capture process of COF-CN and the occurrence of redox reaction, consistent with the thermodynamic findings. To further investigate the state and binding sites of gold ions, X-ray photoelectron spectroscopy (XPS) analysis was conducted before and after gold adsorption on COF-CN. The successful trapping of gold was confirmed by the presence of Au 4f peaks in the XPS spectra following adsorption. The high resolution XPS spectrum of Au 4f revealed peaks at 87.0 and 90.2 eV corresponding to Au(III), while peaks at 85.6 and 89.0 eV were assigned to Au(I), and those at 84.8 and 88.4 eV for contributed to Au(0), respectively (Fig. 4b). The area of the Au(0) peak was larger than those of Au(III) and Au(I) peaks, suggesting the redox reaction is the main adsorption mechanism by which COF-CN achieves gold recovery. The N 1s spectrum following adsorption indicated the presence of C=N and C≡N bonds, with binding energies measured at 398.6 and 399.2 eV. Additionally, a new peak was observed at 400.0 eV, which attributed to $C{=}N^+$ bonds formed through protonation in the acidic solution (Fig. 4c) [25]. The FT-IR and ultraviolet-visible (UV–vis) spectra also proved the existence of the protonated COF-CN (Fig. S9 in Supporting information) [32]. Thus, we infer that the protonating process is the key to gold recovery. In addition, we used the colorimetric method to prove that H_2O_2 was produced in the aqueous solution after adsorption, further confirming the occurrence of redox reactions (Fig. S10 in Supporting information) [33].

The density functional theory (DFT) calculation was employed to better investigate the adsorption mechanism of COF-CN for gold recovery. All DFT calculation details and related parameters can be found in the Supporting information and Table S6 (Supporting information). The interaction energies of COF-CN with $AuCl_4^-$ ($E_{int\text{-}1}$) and COF-CN with $AuCl_4^-$ ($E_{int\text{-}2}$) were calculated, respectively (Figs. 4d and e). It was found that the $E_{int\text{-}2}$ is lower than $E_{int\text{-}1}$ indicating that protonation facilitates stronger interactions between the materials and $AuCl_4^-$. Thus, during the adsorption process the protonated COF-CN is preferentially formed and subsequently combined with $AuCl_4^-$. We proposed the following adsorption mechanism of COF-CN for gold recovery: The process begins with C=N protonation, which is attacked *via* protons from $HAuCl_4$. The protonated C=N then acts as a reducing agent to remove to remove Cl^- from $AuCl_4^-$ to form the intermediate $AuCl_3^{2-}$. Finally, Au ions undergo spontaneous reduction to Au(0) as part of the capture process (Fig. 4f).

The reusability of COF-CN was investigated using a solution containing 0.1 mol/L thiourea and HCl for the desorption of

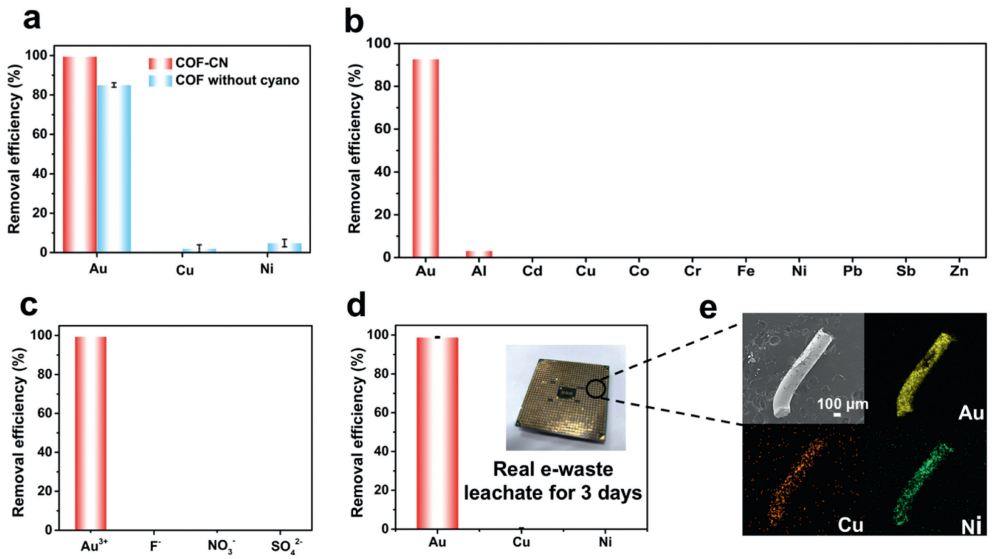


Fig. 5. (a) Comparison of removal efficiency and selectivity between COF-CN and the COF without cyano group. (b, c) Removal efficiency of COF-CN with the existence of various competing cations and anions. (d) Removal efficiency of COF-CN for real e-waste leachate from the CPU immersed in pyridine and NBS for 3 days. (e) The SEM images and energy dispersive spectrometer (EDS) elemental maps from CPU.

Au(III). After five adsorption-desorption cycles, COF-CN consistently achieved a recovery efficiency exceeding 95 %, highlighting its outstanding ability to regenerate and be reused (Fig. S11 in Supporting information).

Furthermore, we investigated the adsorption selectivity of COF-CN for gold. In order to better evaluate the role of cyano functional group, we attempted to synthesize the COF without cyano group under the mild conditions. Unfortunately, the COF without cyano group was difficult to prepare under mild conditions. The solvothermal method was used to prepare the COF without cyano group [34]. A pre-experiment was carried out by adding 200 ppm Au^{3+}, 100 ppm Ni^{2+} and 1000 ppm Cu^{2+} to an acidic aqueous solution to simulate electronic waste leachate. COF-CN not only has a high recovery efficiency, but also has excellent selectivity (Fig. 5a). In addition, we carried out cation and anion interference experiments to better evaluate the selectivity of COF-CN, respectively. COF-CN can achieve highly selective recovery of Au(III) in the presence of various interfering ions while hardly adsorbing other ions (Figs. 5b and c), which can be attributed to the high affinity of $AuCl_4^-$ for the materials and the spontaneous formation of Au(0) nanoparticles during adsorption [35].

The potential of COF-CN for recovering gold from real WEEE samples was investigated. We chose the central processing unit (CPU) as the WEEE source and pretreated them in a more environmentally friendly way using pyridine and N-bromo succinimide. The main ions present in the leaching solution are Au, Cu, and Ni, which is consistent with the EDS analysis of CPU (Fig. 5e). The resulting solution of CPU soaked for 3 days was composed of 367 ppm Cu^{2+}, 189 ppm Ni^{2+}, and 0.34 ppm Au^{3+}. Surprisingly, COF-CN achieved highly selective recovery of gold ions while showing negligible adsorption for Cu and Ni in these actual sample solutions (Fig. 5d). The outstanding selectivity is a result of the large surface area and the introduction of cyano functional group which allow the C=N bond to be protonated more easily, thereby improving the selective capture of gold by the material. The high selectivity of the adsorbent is conducive to obtaining high-purity gold in the end [36].

In this study, we synthesized large-scale cyano-functionalized COFs (COF-CN) under mild conditions. COF-CN exhibits good adsorption performance, and its adsorption mechanism has been clarified. Surprisingly, COF-CN achieves high selectivity and recovery efficiencies for gold ions even in WEEE recovery solutions containing elevated concentrations of competing ions. Furthermore, the cyano group is also an excellent post-modification group. COF-CN can be further modified to an amidoxime and aminophosphonic groups to recover uranyl and rare earth ions.

Declaration of competing interest

The authors declare that they have no known competing financial interests or personal relationships that could have appeared to influence the work reported in this paper.

CRediT authorship contribution statement

Bo Li: Writing – original draft, Visualization, Methodology, Investigation, Formal analysis, Data curation. **Yuanzhe Cheng:** Methodology, Investigation. **Xuyang Ma:** Investigation, Formal analysis. **Dongxu Zhao:** Methodology, Investigation. **Yang Zhang:** Methodology, Investigation, Data curation. **Yongxing Sun:** Methodology, Investigation. **Jia Chen:** Writing – review & editing, Validation, Supervision, Resources, Investigation, Conceptualization. **Li Wu:** Methodology, Investigation. **Liang Zhao:** Investigation. **Hongdeng Qiu:** Validation, Resources, Investigation. **Yujian He:** Writing – review & editing, Supervision, Investigation, Funding acquisition.

Acknowledgment

This work was financially supported by the National Natural Science Foundation of China (No. 51972302).

Supplementary materials

Supplementary material associated with this article can be found, in the online version, at doi:10.1016/j.cclet.2025.111134.

References

[1] R. Kerrich, Science 284 (1999) 2101–2102.
[2] C. Yue, H. Sun, W.J. Liu, et al., Angew. Chem. Int. Ed. 56 (2017) 9331–9335.
[3] E.D. Doidge, I. Carson, P.A. Tasker, et al., Angew. Chem. Int. Ed. 55 (2016) 12436–12439.

[4] O.A. Ogunseitan, Lancet Glob. Health 1 (2013) e313–e314.
[5] X. Chen, Y. Xiang, L. Xu, G. Liu, J. Hazard. Mater. 397 (2020) 122812.
[6] M. Kaya, Waste Manag. 57 (2016) 64–90.
[7] P.E. Karthik, H. Rajan, V.R. Jothi, et al., J. Hazard. Mater. 421 (2022) 126687.
[8] S. Zhong, Y. Wang, T. Bo, et al., Chem. Eng. J. 455 (2023) 140523.
[9] M. Peydayesh, E. Boschi, F. Donat, R. Mezzenga, Adv. Mater. 32 (2024) 2310642.
[10] G.T. Gebremichael, H. Kim, G.M. Nisola, W.J. Chung, Appl. Surf. Sci. 567 (2021) 150743.
[11] F. Li, J. Zhu, P. Sun, et al., Nat. Commun. 13 (2022) 4472.
[12] B. Wang, Y. Ma, W. Xu, K. Tang, J. Hazard. Mater. 451 (2023) 131051.
[13] J. Chen, Y. Wang, Y. Yu, et al., Exploration 3 (2023) 20220144.
[14] J. Xiao, J. Chen, J. Liu, et al., Green Energy Environ. 8 (2023) 1596–1618.
[15] Y. Wang, J. Chen, G. Wang, et al., Sens. Actuators B 359 (2022) 131555.
[16] J. Li, Y. He, Y. Zou, et al., Chin. Chem. Lett. 33 (2022) 3017–3020.
[17] Q. Sun, B. Aguila, L.D. Earl, et al., Adv. Mater. 30 (2018) 1705479.
[18] Z.M. Zhou, W.F. Zhong, K.X. Cui, et al., Chem. Commun. 54 (2018) 9977–9980.
[19] H.L. Qian, F.L. Meng, C.X. Yang, X.P. Yan, Angew. Chem. Int. Ed. 59 (2020) 17607–17613.
[20] J. Qiu, C. Xu, X. Xu, et al., Angew. Chem. Int. Ed. 62 (2023) e202300459.
[21] L. Zhang, Q.Q. Zheng, S.J. Xiao, et al., Chem. Eng. J. 426 (2021) 131865.
[22] M. Liu, D. Jiang, Y. Fu, et al., Angew. Chem. Int. Ed. 63 (2024) e202317015.
[23] L. Guo, Q.Y. Zhang, Z. Yu, et al., Chem. Mater. 35 (2023) 5648–5656.
[24] L. Cusin, H. Peng, A. Ciesielski, P. Samorì, Angew. Chem. Int. Ed. 60 (2021) 14236–14250.
[25] M. Liu, H.-Y. Kong, S. Bi, et al., Adv. Funct. Mater. 33 (2023) 2302637.
[26] Z. Dong, J. Liu, W. Yuan, et al., Chem. Eng. J. 283 (2016) 504–513.
[27] X. Yang, Q. Pan, Y. Ao, et al., Environ. Sci. Pollut. Res. 27 (2020) 38334–38343.
[28] M. Zhao, F. Zhao, J. Ping, et al., Chin. Chem. Lett. 36 (2025) 110782.
[29] K. Li, M. Chen, L. Chen, et al., Environ. Res. 241 (2024) 117588.
[30] B. Li, J. Chen, J. Xiao, et al., ACS Appl. Nano Mater. 6 (2023) 2498–2506.
[31] J. Guo, X. Fan, J. Wang, et al., Chem. Eng. J. 425 (2021) 130588.
[32] J. Yang, A. Acharjya, M.Y. Ye, et al., Angew. Chem. Int. Ed. 60 (2021) 19797–19803.
[33] Y.Z. Cheng, X. Bao, D. Jiang, et al., Angew. Chem. Int. Ed. 64 (2025) e202414943.
[34] M. Yang, C. Mo, L. Fang, et al., Adv. Funct. Mater. 30 (2020) 2000516.
[35] W. Wang, W. Xue, Z. Huang, et al., Chem. Eng. J. 499 (2024) 156667.
[36] W. Wang, M. Wu, W. Xue, et al., Chem. Eng. J. 483 (2024) 149208.